Laser Fabrication and Spectroscopy of Organic Nanoparticles

T. ASAHI,*,† T. SUGIYAMA,‡ AND H. MASUHARA*,‡,§

†Department of Applied Physics, Osaka University, Suita, Osaka 565-0871, Japan, ‡Graduate School of Materials Science, Nara Institute of Science and Technology, Ikoma, Nara 630-0192, Japan, §Department of Applied Chemistry and Institute of Molecular Science, National Chiao Tung University, Hsinchu 30010, Taiwan

RECEIVED ON MAY 19, 2008

CONSPECTUS

In working with nanoparticles, researchers still face two fundamental challenges: how to fabricate the nanoparticles with controlled size and shape and how to characterize them. In this Account, we describe recent advances in laser technology both for the synthesis of organic nanoparticles and for their analysis by single nanoparticle spectroscopy.

Laser ablation of organic microcrystalline powders in a poor solvent has opened new horizons for the synthesis of nanoparticles because the powder sample is converted directly into a stable colloidal solution without additives and chemicals. By tuning laser wavelength, pulse width, laser fluence, and total shot number, we could control the size and

phase of the nanoparticles. For example, we describe nanoparticle formation of quinacridone, a well-known red pigment, in water. By modifying the length of time that the sample is excited by the laser, we could control the particle size (30−120 nm) for nanosecond excitation down to 13 nm for femtosecond irradiation. We prepared β- and γ-phase nanoparticles from the microcrystal with β-phase by changing laser wavelength and fluence. We present further results from nanoparticles produced from several dyes, C_{60}, and an anticancer drug. All the prepared colloidal solutions were transparent and highly dispersive. Such materials could be used for nanoscale device development and for biomedical and environmental applications.

We also demonstrated the utility of single nanoparticle spectroscopic analysis in the characterization of organic nanoparticles. The optical properties of these organic nanoparticles depend on their size within the range from a few tens to a few hundred nanometers. We observed perylene nanoscrystals using single-particle spectroscopy coupled with atomic force microscopy. Based on these experiments, we proposed empirical equations explaining their size-dependent fluorescence spectra. We attribute the size effect to the change in elastic properties of the nanocrystal. Based on the results for nanoparticles of polymers and other molecules with flexible conformations, we assert that size-dependent optical properties are common for organic nanoparticles. While "electronic confinement" explains the size-dependent properties of inorganic nanoparticles, we propose "structural confinement" as an analogous paradigm for organic nanoparticles.
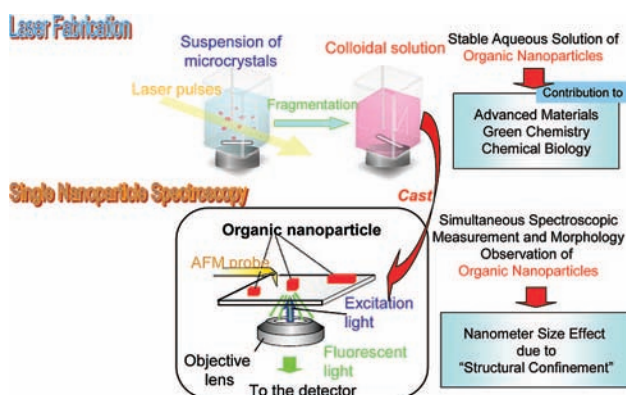
1. Introduction

When the size of materials is reduced from bulk to micrometer and from micrometer to nanometer, physical and chemical properties are expected to change, and indeed the thermal, electric, and elec-tronic properties of metals and semiconductors are examined as a function of the size. In contrast, such studies have not been conducted so much for organic molecular solids, because it has been believed that the size effect is not expected

because electrons are confined in each molecule and do not expand over the nanometer and micrometer domains. Furthermore most of chemists had no "size" concept before microchemistry studies were started.[1,2] Now we know chemistry in nanometer dimensions is important, and studies on organic nanoparticles are expected to bridge gaps between the understanding of molecules and materials.

Practically, organic nanoparticles are being used as advanced materials such as display elements, inks, toners, drugs, cosmetics, and so on, and in the future, they could be considered to contribute to wider fields of chemistry and material science. The first step in the nanoparticle research is how to fabricate the nanoparticles with the requested size and shape. Microparticles of organic molecules have been traditionally fabricated by mechanical milling treatments; however their size is usually over sub-micrometer. To obtain smaller nanoparticles, many trials have been done at laboratory scale, and several effective ways have been developed. In 1992, Nakanishi and co-workers proposed the reprecipitation method and demonstrated the nanoparticles with the particle size less than 100 nm dispersed in water,[3] and since then, this method has been widely used in nanoparticle preparation for various kinds of molecules.[4-15] Another approach to nanoparticle preparation based on controlling precipitation of the molecule is to use the sol−gel phase transition,[16] solvent evaporation in polymer solution,[17,18] and stratification deposition in a vacuum chamber.[19,20] Because the above methods are based on the molecular association under some mixing, evaporation, or cooling conditions, it is not so easy to control the size, shape, and phase of the nanoparticles in their preparation processes. From this viewpoint, we have proposed and developed a new fabrication method of organic nanoparticles utilizing laser ablation of microcrystals in water, where the bulk solids are converted directly into nanoparticles. We summarize the laser ablation method and discuss its great potential in nanoscience and nanotechnology in this Account.

The other key step in nanoparticle research is how to characterize nanoparticles. In general, nanoparticles are measured and analyzed as an ensemble, and unique size-dependent optical properties, which are different from those of metals and semiconductors, have been reported. Because some properties characteristic of nanometer dimension may be hidden in the ensemble-averaged data, single-particle spectroscopy giving various properties as functions of the nanoparticle size, shape, and crystalline phase is strongly desired. Here size-dependent optical properties are also summarized, and the important role of single-nanoparticle spectroscopy is demonstrated.
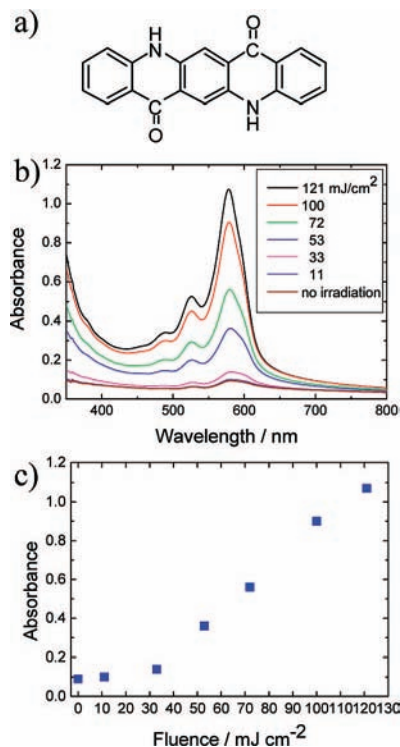

FIGURE 1. (a) A chemical structure of quinacridone (QA), (b) absorption spectra of supernatants of QA colloidal solutions obtained at various laser fluences, and (c) the plot of absorbance at 580 nm as a function of laser fluences.

2. Fabrication of Nanoparticles by Laser Ablation in Solvent

When organic microcrystals are suspended in water and exposed to intense laser pulses, fragmentation of the microcrystals is induced. The ejected particles are caught by water and stabilized as nanocolloids.[21-26] We proposed this laser ablation method in 2000 and have examined its applicability and studied its mechanism.[21-24] First we describe some results on quinacridone (QA, Figure 1a) as a representative example to explain the method.[24]

Microcrystalline powder of QA obtained by hand-grinding of bulk crystal in an agate mortar was suspended in water, and then the mixture was irradiated with 355 nm nanosecond laser pulses (8 ns fwhm and 10 Hz repetition rate). The absorption spectra of the supernatants before and after laser irradiation at various laser fluences are shown in Figure 1b, and the absorbance at 580 nm is plotted as a function of the laser fluence in Figure 1c. The spectra indicate that QA is barely dissolved in water, while the fluence dependence means that its formation has a threshold with respect to the laser fluence. We took out a droplet of the red supernatant, deposited it on a silicon substrate, and observed the nanoparticles with SEM. The SEM image prepared at 100 mJ/cm² is shown in Figure 2a, and the mean size is estimated to be 50
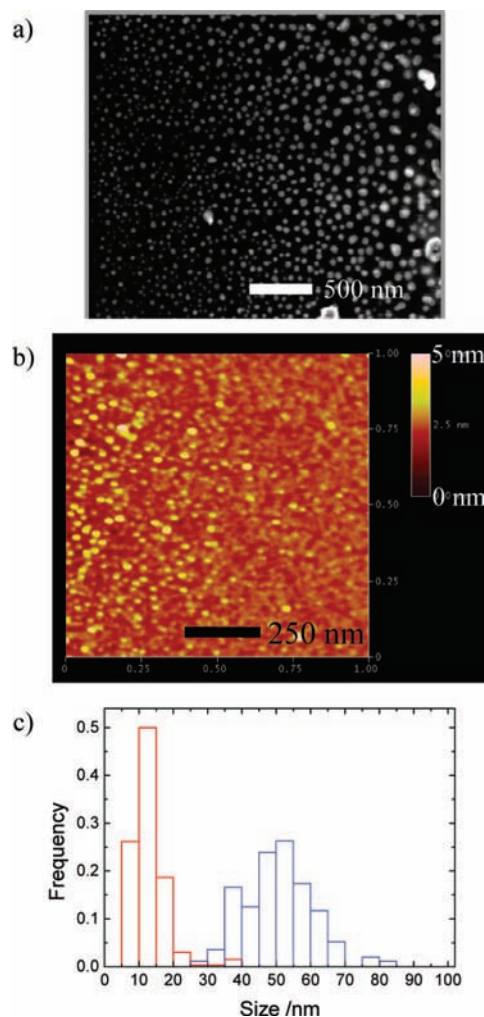
FIGURE 2. (a) A SEM image of QA nanoparticles formed by nanosecond laser irradiation (8 ns, 355 nm) at 100 mJ/cm², (b) AFM image of QA nanoparticles formed by femtosecond laser irradiation (150 fs, 800 nm) at 40 mJ/cm², and (c) The size histograms of QA nanoparticles formed by femtosecond (red) and nanosecond (blue) laser irradiation.

nm, and its standard deviation is 10 nm. The size reduction during laser ablation was monitored by measuring absorption and light scattering of the colloid, and we understood how the mean particle size became smaller and the distribution narrower.[23c] On the basis of the results, it is concluded that QA nanoparticles are fabricated by laser ablation in water.

Similarly we examined a series of dye molecules similarly to the procedure for QA, and the obtained results are listed in Table 1.[22–24] The threshold for nanoparticle formation is in the fluence range from 6 to 30 mJ/cm² depending on dye molecules, while their particle size is around 50 nm, almost independent of dyes when the nanoparticles were prepared at laser fluence three times larger than the threshold. All the prepared colloid solutions were transparent and highly dispersive, and their half-life covered from a few days to 2 months.

It is considered that laser ablation of organic microcrystals in poor solvent is an easy, useful, and general method for fabricating their nanoparticles.

One advantage of the laser ablation method is its high controllability of size and phase of nanoparticles by tuning laser pulse width, wavelength, fluence, and shot number. In Table 2, some results obtained for QA are listed,[23,24] and the AFM image of nanoparticles and the size distribution are given in Figure 2b,c, respectively. Higher fluence led to smaller nanoparticles, and the size changed drastically depending on pulse width.[24] It is especially worth noting that we have succeeded in the fabrication of 13 nm size QA nanoparticles by femtosecond laser irradiation.[23c,d] Another interesting result is that the phase of the formed QA nanoparticles depends on laser wavelength and fluence. Judging from absorption spectra of the nanocolloidal solution, β-phase was always produced for 355 nm excitation, while β- and γ-phase nanoparticles were formed at 532 and 580 nm excitation wavelengths, where QA has a larger absorption coefficient than that at 355 nm.[23a]

These dependences on laser parameters can be explained in terms of the laser ablation mechanism: photothermal for nanosecond laser ablation[27a–c] and photomechanical for femtosecond ablation.[27d] These mechanisms were concluded on the basis of time-resolved fluorescence and absorption spectroscopy, dynamic imaging, and related optical measurement during the laser irradiation. For nanosecond photothermal ablation in a solvent, rapid temperature elevation upon pulse excitation is compensated by a cooling process due to thermal diffusion to the solvent, and its balance gives the transient temperature determining the nanoparticle size.[23a,24] Higher fluence gives higher effective transient temperature, leading to efficient fragmentation to smaller particles. In the case of femtosecond irradiation, multiphoton absorption leads to very rapid increase in molecular and lattice vibrations giving transient high pressure in the irradiated area.[27d] As a result explosive mechanical fragmentation is started before thermal equilibrium with the solvent, leading to the small nanoparticles.

The fluence dependence of the phase of the formed QA nanoparticles is consistent with its thermodynamic stability. It is well-known that γ-phase is a little more stable than β-phase, while their interconversion is difficult at room temperature because some energy barrier exists between two phases.[28] In our case, β-phase QA microcrystal is ablated in water, and nanoparticles with β- and γ-phases are prepared just above the threshold fluence of laser ablation and at higher fluence, respectively. This is quite acceptable because the interconver-

TABLE 1. Dye Nanoparticles Prepared by Nanosecond Laser Ablation of Microcrystalline Powders in Poor Solvent[a]

	BY	AlPc	BP	DR	QA	VOPc
mean size (nm) ± standard deviation (nm)	59 ± 16	56 ± 28	40 ± 9	43 ± 10	50 ± 10	49 ± 15
threshold (mJ cm^{-2})	8	6	10	7	30	20
stability of colloidal dispersion[b]	13 days	2 months	6 days	6 days	20 days	5 days

[a] Excitation light is the third harmonic (355 nm) of a nanosecond Nd^{3+}:YAG laser (8 ns fwhm, 10 Hz) or a XeCl excimer laser (351 nm, 30 ns FWHM, 10 Hz). Abbreviations: BY = 3,3′-dichloro-4,4′-[2-oxo-1-(*N*-phenylcarbamoyl) propylazo]-1,1′-biphenyl; AlPc = aluminum phthalocyanine chloride; BP = 6,6′-dichloro-4,4′-dimethylth; DR = 3-hydroxy-4-[(4-methyl-2-nitrophenyl)azo]-*N*-(3-nitrophenyl)-2-naphthalenecarboxamide; QA = quinacridone; VOPc = oxo(phtalocyaninato)vanadium(IV). [b] The half-decay time of the absorbance of colloidal dispersion.

TABLE 2. Crystal Phase and Size of Quinacridone Nanoparticles Fabricated by Laser Ablation by Choosing Laser Parameters

	laser parameters: wavelength (pulse width)	fluence (mJ/cm^2)				
		25	40	80	100	150
mean particle size, nm (crystalline phase)	355 nm (8 ns)		120 (β)	68 (β)	50 (β)	30 (β)
	532 nm (8 ns)		110 (β)	55 ($\beta+\gamma$)	35 ($\beta+\gamma$)	25 (γ)
	580 nm (8 ns)		(β)		22 (γ)	
	800 nm (150 fs)	40 (β)	13 (β)		(γ)	

sion from β-phase to γ-phase needs additional energy during ablation.

3. Size-Dependent Optical Properties of Organic Nanoparticles

It is well-known that optical spectroscopy of metal and inorganic semiconductor nanoparticles show typical nanometer size dependences, which can be ascribed to electron confinement in small volumes.[29] However, the electron confinement effect is not expected for organic crystals, since electrons are localized only in chemical bonds or just over one molecule. Nevertheless, organic nanoparticles show interesting size effects of absorption and fluorescence spectra, fluorescence emission enhancement,[12,13] and nonlinear optical response.[30] Many papers have considered size-dependent optical properties of organic nanoparticles and reported that their size domain is quite different from that of inorganic materials, covering from a few tens of nanometers to a few hundreds of nanometers.[4−7,11,31−35]

Kasai et al. reported that perylene nanocrystals gave monomer and excimer emissions and that the latter peak wavelength showed a blue shift and the monomer emission was enhanced.[6] Similar dual emission behavior was also observed by Seko et al. for pyrene, corone, and anthracene, and it was explained by assuming two emissive centers; one is in the inner side and the other is at the periphery of the nanoparticle.[20] Matsui and his colleagues examined aromatic nanocrystals in polymer films and found that the absorption bandwidth increased with size but showed a sudden fall to zero over 12 nm.[31] To explain this novel phenomenon, they made theoretical consideration by taking into account the effect of surface charge.

More complex luminescence phenomena of nanoparticles were reported by Park et al. for 1-cyano-*trans*-1,2-bis-(4′-methylbiphenyl)ethylene[13] and by Patra et al. for 7,7-bis(4-chloroanilinol)-8,8-dicyanoquinodimethane,[32] and a systematic study was extended by Yao and his colleagues for nanoparticles of pyrazoline derivatives such as 1,3-diphenyl-5-(2-anthryl)-2-pyrazoline.[33] Those nanoparticles gave multiple emissions involving charge-transfer luminescence and showed that the fluorescence spectra differed from those of bulk solid and solution. Because these molecules have flexible conformations, various inter- and intramolecular overlapping structures are realized in nanoparticles, depending on the particle size and shape. A similar geometrical effect of molecular packing in a confined space was also discussed for a cyanine *J*-aggregate.[34]

In the case of conjugated polymers, more distinct size dependence is expected because polymer chains are longer and their conformations are more flexible. We studied poly(3-[2-(*N*-dodecylcarbamoyloxy)ethyl]-thiophene-2,5-diyl)[35] and confirmed such size-dependent absorption and fluorescence spectra in the size range of a few tens to a few hundreds of nanometers. For poly[2-methoxy,5-(2′-ethyl-hexyloxy)-*p*-phenylene vinylene], the fluorescence properties including the dynamics of exciton migration, trapping, and quenching have been investigated by Barbara et al.,[36] and the size-dependent fluorescence was discussed from the viewpoints of conformational order and heterogeneity of polymer chains confined by the nanometer dimension.
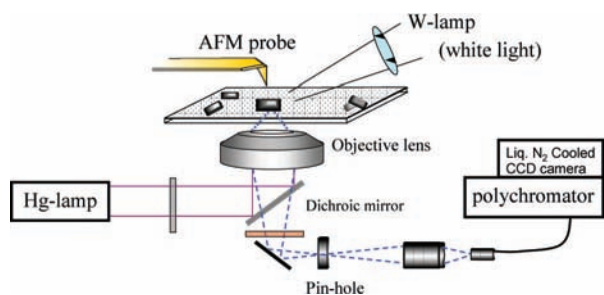
FIGURE 3. An experimental setup for single-particle spectroscopy coupled with AFM observation.

4. Single Nanocrystal Spectroscopy of Perylene

Most of the above studies have been done by ensemble measurement of the colloidal solution, so the size-dependent spectra are averaged over different sizes and shapes. Furthermore, it is possible that nanoparticles contain some amorphous or polymorphous domains and are even contaminated with solvent. Therefore, it has been strongly desired to reveal simultaneously optical properties and morphology for individual nanoparticles under dry conditions. In the past decade, several works using single-nanoparticle spectroscopy have been reported for organic nanoparticles.[36−47] As a representative molecular nanocrystal, perylene was first examined by single-nanocrystal spectroscopy using a near-field optical setup, but the size dependence of the fluorescence spectra was not made clear.[43,44] Some groups and we have developed experimental setups for far-field microspectroscopy combined with AFM observation.[38−42] Figure 3 shows a schematic illustration of our far-field fluorescence/light scattering microspectroscope coupled with an AFM. From the top, AFM observation is conducted, while optical measurement is performed from the bottom. By applying this to single organic nanoparticles on a dried surface and by examining the relation between their morphologies and optical spectra, we have elucidated the intrinsic nature of the size-dependent optical spectra.

Figure 4 shows some examples of the AFM images and fluorescence spectra of single perylene nanocrystals.[40] A broad excimer emission around 600 nm and a monomer fluorescence peak at 480 nm were detected for each crystal, while the spectrum changed from nanocrystal to nanocrystal. We examined many nanocrystals and tried to relate the peak wavelength of the excimer emission and the intensity ratio of the monomer over excimer peaks to size parameters. The spectrum did not show any clear dependence on the height, width, and length of each nanocrystal. Instead we found that the "size" defined by eq 1 can be related to the fluorescence spectroscopic data.

$$size = \sqrt[3]{length \times width \times height} \qquad (1)$$

We consider the mechanism of the present size dependence by referring to the fluorescent nature of the α-form bulk perylene crystal,[48,49] which is explained in terms of the strong coupling model of short-range exciton−phonon (lattice vibration) interaction.[50] In the case of α-form crystal, because the lattice relaxation energy (E_{LR}) is large enough, electronic excitation energy is trapped in a sandwich-like pair of two molecules, that is, excimer formation. With use of a generalized configuration coordinate Q, E_{LR} is given by $E_{LR} = \omega Q_m^2/2$, where ω is the angular frequency of the phonon and Q_m means a relative displacement of the excimer state from the bottom of the ground state. Our consideration is schematically illustrated in Figure 5, where self-trapping energy (E_{ST}) is given by $E_{ST} = E_{LR} - B$ and B is half of the free exciton bandwidth. The fluorescence peak energy of excimer emission, hc/λ_{max}^E, is presented by $hc/\lambda_{max}^E = hc/\lambda_{max}^M - E_{ST} - \Delta E_g$, where ΔE_g means the Franck−Condon destabilization energy in the ground state. On the other hand, it is well-known that the monomer fluorescent state is thermally in equilibrium with the excimer state,[48] and the intensity ratio of the monomer over the excimer, I_M/I_E, is given by

$$I_M/I_E = k_M/k_E \exp(-E_{ST}/(kT)) \qquad (2)$$

where k_M and k_E are the radiative transition rate constants from the monomer and excimer states to the ground state, respectively.

Because the monomer fluorescence peak of nanocrystal is identical to that of the bulk one, the value of B can be considered to be independent of size. Therefore, the size dependences of λ_{max}^E and I_M/I_E should be ascribed to reduction in E_{LR}
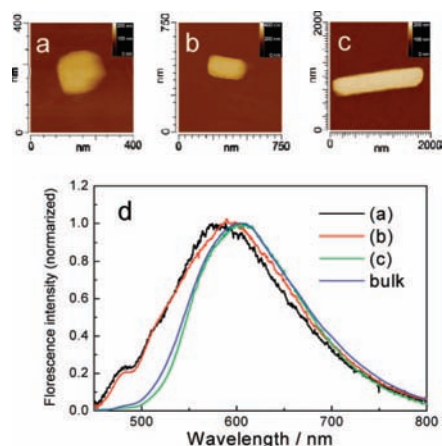

FIGURE 4. (a−c) AFM images of perylene nanocrystals and (d) fluorescence spectra corresponding to the AFM images in panels a−c and that of a bulk crystal (blue line). All the spectra were corrected with respect to the spectral sensitivity of the instrument and were normalized to unity at the maximum intensity.
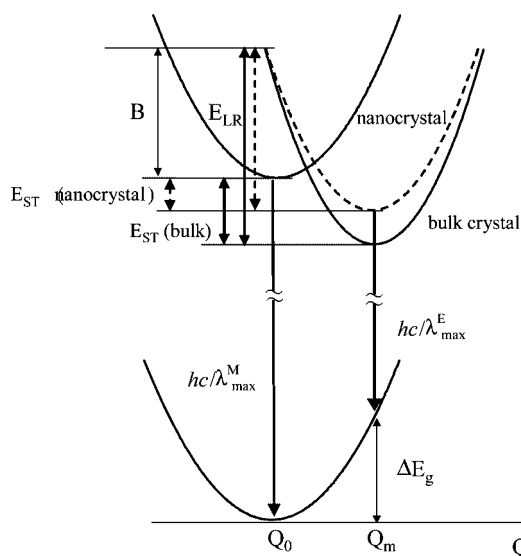
FIGURE 5. Schematic illustration of potential energy surfaces of perylene nano- and bulk crystals. It assumed that the ground and excited Franck–Condon states give the same potential to bulk crystal. Abbreviations are in the text.
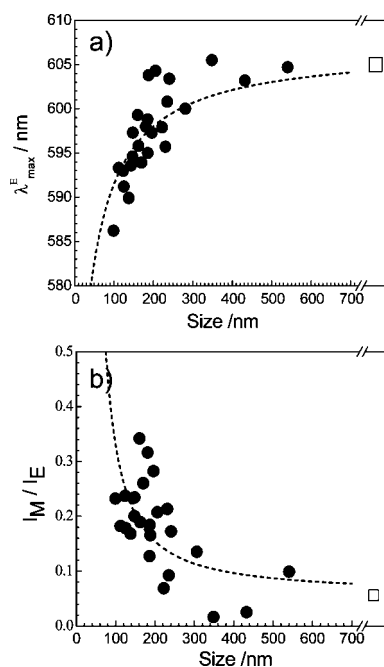

FIGURE 6. (a) Dependence of the excimer fluorescence peak on size and (b) dependence of the intensity ratio of monomer to excimer emissions at their peaks on size. Size is defined by eq 1. Dotted lines in panels a and b represent the calculated size dependences of λ^E_{max} from eq 4 and of I_M/I_E from eqs 2 and 3 using $a = 34$ nm (see text).

with the decrease in the size. Because E_{LR} is a function of the angular phonon frequency of crystalline lattice and lattice distortion due to excimer formation, the present size effect can be attributed to a change in elastic properties of nanocrystal with size. We have considered that the lattice instability caused by the large surface-to-volume ratio will be responsible for lowering of lattice vibration or rigidity with the decrease in the crystal size, which leads to the up-shift of the excimer energy level.[40a] Indeed, it was confirmed experimentally that hc/λ^E_{max} increases monotonously with the surface-to-volume ratio, and its relation looked roughly linear. This idea will be related to the fact that the melting temperature of metallic nanoparticles and some organic nanocrystals is lower than that of bulk, which is eventually ascribed to the increase in free energy of the nanocrystal by a contribution of the surface free energy.[51−53]

Along this line, we proposed the following empirical equations as a function of size as defined by eq 1 by assuming that the lattice relaxation energy in the nanocrystal decreases linearly with the surface-to-volume ratio, that is, the inverse of size,[40a]

$$E_{ST}(\text{nanocrystal}) = E_{ST}(\text{bulk}) - b/(\text{size} + a) \qquad (3)$$

$$hc/\lambda^E_{max}(\text{nanocrystal}) = hc/\lambda^E_{max}(\text{bulk}) + b/(\text{size} + a) \qquad (4)$$

where a is a parameter having the distance dimension $b = aE^{bulk}_{LR}$, and ΔE_g is set to be constant in the derivation of eq 4. Using the value of lattice relaxation energy in bulk, E^{bulk}_{LR} (1715 cm^{-1}),[48] we calculated the size dependence of λ^E_{max} from eq

4 and the dependence of I_M/I_E from eqs 2 and 3, by assuming k_M/k_E to be independent of the size. As shown in Figure 6, the calculated size dependences both for λ^E_{max} and I_M/I_E can reproduce the experimental results semiquantitatively when the value of a is about 30 nm. The physical meaning of the value of a might be related to structural homogeneity of the nanocrystal but is not so clear at the present stage of investigation. This is the first work to propose empirical equations representing size-dependent optical spectra of organic nanocrystals as far as we know, and such trials are strongly desired for understanding the nature of the optical properties. Single-nanoparticle spectroscopic study on organic systems has a short history, so further systemic studies on the nanosize effect should be extended in more detail. There is no doubt that single-nanoparticle/nanocrystal spectroscopy with AFM observation is very useful and provides novel results.

5. Structural Confinement in Organic Nanoparticles Giving Unique Size Effects

In addition to the size effect of the perylene nanocrystal, which can be explained by a change of elastic properties of the crystal, we here point out other effects on the size-dependent optical properties of organic nanoparticles. As described in section 3, conformational structures of molecules confined in a small

space are the key issue to explain the size dependence of nanoparticle fluorescence in the case of flexible molecules, especially conjugated polymers. Morphological effects of polymer chains such as a chain packing, conformational defects, and distortions were also presented for understanding single nanocrystal Rayleigh scattering spectroscopy of poly(substituted diacetylene).[38,39] The excitonic transition resonance peak can be correlated to the cross section of nanocrystals with a rectangular shape, which is ascribed to mutual coupling of electronic polarization in the bundle of the chains or to conformational instability giving defects and kinks. On the basis of the spectroscopic data of various organic compounds, we can conclude that the size effect on organic nanoparticles is characteristic of a few tens and a few hundreds of nanometers order and related to some molecular conformation, packing, and elastic properties of nanoparticles. This gives us the idea to call the present size effect "Structural Confinement", is contrast to electron confinement for metals and inorganic semiconductors.

6. Future Potential of Organic Nanoparticles

As a summary of this Account, we discuss the great potential of organic nanoparticles in green chemistry and chemical biology. Organic nanoparticles can be dispersed well in water, so studies on their chemical reactions will not always need organic solvents. The larger surface of nanoparticles may give a greater chance for them to encounter other reactants than bulk solids, a chemical reaction might proceed at the colliding surfaces. These are consistent with the requirements for green chemistry, where water is preferred to organic solvents from the viewpoint of health and environmental concerns.[54] The excellent solubility of organic nanoparticles in water will also open new aspects also in chemical biology. Usually chemical modification or dispersion by adding detergents are applied to dissolve organic molecules and to react them with living cells, but their nanoparticles can interact with living cells and tissues without such treatments.

To achieve such status of organic nanoparticles, their size, shape, and phase should be controlled fully, which will be realized by developing the laser ablation method. This is one of the top-down methods of nanoparticle fabrication, where no contamination is involved because no solvent is added, the process is in principle noncontact, and the nanoparticles can be collected in poor solvent without being exposed to air. As examples, we here introduce laser fabrication of C_{60} fullerene[55,56] and an anticancer drug. C_{60} has recently attracted increased interest in its medical application such as a novel photodynamic therapy drug. We prepared the aqueous colloid with size 30−50 nm by laser ablation.[55] The colloid is stable without detergents and organic solvents, so this is one of the best samples for the use of C_{60} in its medical and biological applications. 7-Ethyl-10-hydroxycamptothencin, on the other hand, is well-known as a candidate drug for cancer therapy, but does not dissolve well in water. This molecule was also successfully fabricated as an aqueous nanocolloid by laser ablation, and its interaction with living cells was tested. The effect as a drug was proven to be acceptable enough and lasted longer with a lower amount than expected. These examples indicate great potential of organic nanoparticles and give us a dream where nanoparticles are key materials in innovative research fields of chemistry. Spectroscopic analysis of nanoparticles is also important and indispensable for characterization and functionalization. The ultimate potential of the relevant optical and chemical properties will be shown by single-nanocrystal spectroscopy.

BIOGRAPHICAL INFORMATION

Tsuyoshi Asahi received his B. Sc. and Ph.D. from Osaka University under Professor Noboru Mataga. At Osaka University his thesis focused on the dynamics and mechanism of photoinduced electron transfer in solution. In 1991 he joined Masuhara Microphotoconversion Project (ERATO, JST) as Researcher, and in 1992 he moved to Department of Applied Physics at Osaka University as Research Associate. He was promoted to Associate Professor at the Department in 1999. He has been interested in the dynamics of laser-induced chemistry of organic molecules in solids. Recent topics include the fabrication of organic nanoparticles, the spectroscopic properties of organic and noble metal nanoparticles, and their hybrid metal/molecule nanostructures.

Teruki Sugiyama received his Ph.D. from Nankai University, P. R. China, in 2002. He was Postdoctoral Fellow and appointed Assistant Professor in the Department of Applied Physics at Osaka University under the supervision of Professor Hiroshi Masuhara, where he studied the preparation of organic nanoparticles utiliz-

ing laser ablation in solution 2002−2006. Then he became Researcher at Hamano Life Science Research Foundation in 2007 and is currently studying a new topic in laser trapping crystallization at Nara Institute of Science and Technology.

Hiroshi Masuhara graduated from Tohoku University in Sendai in 1966 and received his Ph.D. in 1971 at Osaka University, where his mentors were the late Professor Masao Koizumi and Professor Noboru Mataga, respectively. He worked in the Mataga laboratory at Osaka University till 1984 and then had his own laboratory in Kyoto Institute of Technology, Osaka University, and then Hamano Life Science Research Foundation, while he was also the director of ERATO Masuhara Microphotoconversion Project, JST, 1988−1993. Now he is extending his research at Nara Institute of Science and Technology and National Chiao Tung University in Taiwan, where his group is developing new laser-microscope methodologies for bio/nanosciences and understanding laser-induced crystallization of molecules and proteins.

FOOTNOTES

REFERENCES

1 *Microchemistry: Chemistry and Spectroscopy in Small Domains*; Masuhara, H., De Schryver, F. C., Kitamura, N., Tamai, N., Eds.; North-Holland: Amsterdam, 1994.

2 *Mesoscopic Organic Chemistry*; Masuhara, H., De Schryver, F. C., Eds.; Blackwell Science: Oxford, U.K., 1999.

3 Kasai, H.; Nalwa, H. S.; Oikawa, H.; Okada, S.; Matsuda, H.; Minami, N.; Kakuta, A.; Ono, K.; Mukoh, A.; Nakanishi, H. A Novel Preparation Method of Organic Microcrystals. *Jpn. J. Appl. Phys.* **1992**, *31*, L1132–L1134.

4 Kasai, H.; Oikawa, H.; Okada, S.; Nakanishi, H. Crystal Growth of Perylene Microcrystals in the Reprecipitation Method. *Bull. Chem. Soc. Jpn.* **1998**, *71*, 2597–2601.

5 Kasahi, H.; Nalwa, H. S.; Okada, S.; Oikawa, H.; Nakanishi, H. *Handbook of Nanostructured Materials and Nanotechnology*; Academic Press: New York, 2000; Vol. 5,Chapter 8, pp 433−473.

6 Katagi, H.; Kasai, H.; Okada, S.; Oikawa, H.; Komatsu, K.; Matsuda, H.; Liu, Z.; Nakanishi, H. Size Control of Polydiacetylene Microcrystals. *Jpn. J. Appl. Phys.* **1996**, *35*, L1364–L1366.

7 Horn, D.; Rieger, J. Organic Nanoparticles in the Aqueous Phase—Theory, Experiment, and Use. *Angew. Chem., Int. Ed.* **2001**, *40*, 4330–4361.

8 Lee, J.-K.; Koh, W.-K.; Chae, W.-S.; Kim, Y.-R. Novel Synthesis of Organic Nanowires and their Optical Properties. *Chem. Commun.* **2002**, *138*, 139.

9 Fujita, S.; Kasai, H.; Okada, S.; Oikawa, H.; Fukuda, T.; Matsuda, H.; Tripathy, S. K.; Nakanishi, H. Electric-Field-Induced Orientation of Organic Microcrystals with Large Dipole Moment. *Jpn. J. Appl.Phys.* **1999**, *38*, 659–661.

10 Fortner, J. D.; Lyon, D. Y.; Sayes, C. M.; Boyd, A. M.; Falkner, J. C.; Hotze, E. M.; Alemany, L. B.; Tao, Y. J.; Guo, W.; Ausman, K. D.; Colvin, V. L.; Hughes, J. B. C$_{60}$ in Water: Nanocrystal Formation and Microbial Response. *Environ. Sci. Technol.* **2005**, *39*, 4307–4316.

11 Fu, H.; Yao, J. Size Effects on the Optical Properties of Organic Nanoparticles. *J. Am. Chem. Soc.* **2001**, *123*, 1434–1439.

12 Li, S.; He, L.; Xiong, F.; Li, Y.; Yang, G. Enhanced Fluorescent Emission of Organic Nanoparticles of an Intramolecular Proton Transfer Compound and Spontaneous Formation of One-Dimensional Nanostructures. *J. Phys. Chem. B* **2005**, *108*, 10887–10892.

13 An, B. K.; Kwon, S. K.; Jung, S. D.; Park, S. Y. Enhanced Emission and its Switching in Fluorescent Organic Nanoparticles. *J. Am. Chem. Soc.* **2002**, *124*, 14410–14415.

14 Baba, K.; Kasai, H.; Okada, S.; Oikawa, H.; Nakanishi, H. Novel Fabrication Process of Organic Microcrystals Using Microwave-Irradiation. *Jpn. J. Appl. Phys.* **2000**, *39*, L1256–L1258.

15 Komai, Y.; Kasai, H.; Hirakoso, H.; Hakuta, Y.; Katagi, H.; Okada, S.; Oikawa, H.; Adschiri, T.; Inomata, H.; Arai, K.; Nakanishi, H. Preparation of Organic Microcrystals Using Supercritical Fluid Crystallization Method. *Jpn. J. Appl. Phys* **1999**, *38*, L81–L83.

16 Ibanez, A.; Maximov, S.; Guiu, A.; Chaillout, C.; Baldeck, P. L. Controlled Nanocrystallization of Organic Molecules in Sol-Gel Glasses. *Adv. Mater.* **1998**, *10*, 1540–1543.

17 Ye, J.; Chen, H.-Z.; Wang, M. Preparation and Characterization of Chloroindium Phthalocyanine Nanoparticles from Complexation-Mediated Solubilization. *J. Mater. Sci.* **2003**, *38*, 4021–4025.

18 Matsui, A. H.; Mizuno, K.; Nishi, O.; Matsushima, Y.; Shimizu, M.; Goto, T.; Takeshima, M. Densities of States and Band Widths of Excitons in Anthracene Microcrystallites Embedded in PMMA. *Chem. Phys.* **1995**, *194*, 167–174.

19 Toyotama, H. Water Dispersion Containing Ultrafine Particles of Organic Compounds US Patent 5,354,563, 1994.

20 Seko, T.; Ogura, K.; Kawakami, Y.; Sugino, H.; Toyotama, H.; Tanaka, J. Excimer Emission of Anthracene, Perylene, Coronene and Pyrene Microcrystals Dispersed in Water. *Chem. Phys. Lett.* **1998**, *291*, 438–444.

21 Tamaki, Y.; Asahi, T.; Masuhara, H. Tailoring Nanoparticles of Aromatic and Dye Molecules by Excimer Laser Irradiation. *Appl. Surf. Sci.* **2000**, *168*, 85–89.

22 (a) Tamaki, Y.; Asahi, T.; Masuhara, H. Nanoparticle Formation of Vanadyl Phthalocyanine by Laser Ablation of Its Crystalline Powder in a Poor Solvent. *J. Phys. Chem. A* **2002**, *106*, 2135–2139. (b) Tamaki, Y.; Asahi, T.; Masuhara, H. Solvent-Dependent Size and Phase of Vanadyl Phthalocyanine Nanoparticles Formed by Laser Ablation of VOPc Crystal-Dispersed Solution. *Jpn. J. Appl. Phys.* **2003**, *42*, 2725–2729.

23 (a) Sugiyama, T.; Asahi, T.; Takeuchi, H.; Masuhara, H. Size and Phase Control in Quinacridone Nanoparticle Formation by Laser Ablation in Water. *Jpn. J. Appl. Phys.* **2006**, *45*, 384–388. (b) Jeon, H.-G.; Sugiyama, T.; Masuhara, H.; Asahi, T. Study on Electrophoretic Deposition of Size-Controlled Quinacridone Nanoparticles. *J. Phys. Chem. C* **2007**, *111*, 14658–14663. (c) Sugiyama, T.; Takeuchi, H.; Asahi, T.; Yoshikawa, Y. H.; Hosokawa, Y.; Masuhara, H. Laser Fabrication of Nanoparticles and Crystals in Solution. Proceedings of the 3rd Pacific International Conference on Application of Lasers and Optics; 2008, 807812. (d) Sugiyama, T.; Asahi, T.; Masuhara, H. Formation of 10 nm-sized Oxo(phtalocyaninato) Vanadium (IV) Particles by Femtosecond Laser Ablation in Water. *Chem. Lett.* **2004**, *33*, 724–725.

24 (a) Asahi, T.; Yuyama, K.; Sugiyama, T.; Masuhara, H. Preparation of Organic Dye Nanoparticles by Nanosecond Laser Ablation in a Poor Solvent. *Rev. Laser Eng. (in Japanese)* **2005**, *33* (1), 41–46. (b) Sugiyama, T.; Asahi, T.; Yuyama, K.; Takeuchi, H.; Jeon, H. G.; Hosokawa, Y.; Masuhara, H. Laser Fabrication and Crystallization of Nano Materials. *Proc. SPIE* **2008**, *6891*, 689112_1–689112_8.

25 Kita, S.; Masuo, S.; Machida, S.; Itaya, A. Nanoparticle Formation of Pentacene by Laser Irradiation in Ethanol Solution. *Jpn. J. Appl. Phys.* **2006**, *45*, 6501–6507.

26 Li, B.; Kawakami, T.; Hiramatsu, M. Enhancement of Organic Nanoparticle Preparation by Laser Ablation in Aqueous Solution Using Surfactants. *Appl. Surf. Sci.* **2003**, *210*, 171–176.

27 (a) Fukumura, H.; Masuhara, H. The Mechanism of Dopant-induced Laser Ablation Possibility of Cyclic Multiphoton Absorption in Excited States. *Chem. Phys. Lett.* **1994**, *221*, 373–378. (b) Fujiwara, H.; Fukumura, H.; Masuhara, H. Laser Ablation of a Pyrene-Doped Poly(methyl methacrylate) Film: Dynamics of Pyrene Transient Species by Spectroscopic Measurements. *J. Phys. Chem.* **1995**, *99*, 11844–11853. (c) Fujiwara, H.; Hayashi, T.; Fukumura, H.; Masuhara, H. Each Dopant Can Absorb More than Ten Photons. Transient Absorbance Measurement at Excitation Laser Wavelength in Polymer Ablastion. *Appl. Phys. Lett.* **1994**, *64*, 2451–2453. (d) Hosokawa, Y.; Yashiro, M.; Asahi, T.; Masuhara, H. Photothemal Conversion Dynamics in Femtosecond and Picosecond Discrete Laser Etching of Cu-Phthalocyanine Amorphous Film Analyzed by Ultrafast UV-VIS Absorption Spectroscopy. *J. Photochem. Photobiol. A* **2001**, *142*, 197–207.

28 Ganryonojiten; Ito, S., Ed.; Asakura Publishing: Tokyo, Japan, 2000; Chapter 4 (in Japanese).

29 (a) Steigerwald, M. L.; Brus, L. E. Semiconductorcrystallites: A Class of Large Molecules. *Acc. Chem. Res.* **1990**, *23*, 183–188. (b) Burda, C.; Chen, X.; Narayanan, R.; El-Sayed, M. A. Chemistry and Properties of Nanocrystals of Different Shapes. *Chem. Rev.* **2005**, *105*, 1025–1102.

30 (a) Treussart, F.; Botzung-Appert, E.; Ha-Duong, N.-T.; Ibanez, A.; Roch, J.; Pansu, R. Second Harmonic Generation and Fluorescence of CMONS Dye Nanocrystals Grown in a Sol-Gel Thin Film. *ChemPhysChem* **2003**, *4*, 757–760. (b) Tian, Z.; Huang, W.; Xiao, D.; Wang, S.; Wu, Y.; Gong, Q.; Yang, W.; Yao, J. Enhanced and Size-Tunable Third-Order Nonlinearity of Nanoparticles from an Azo Metal Chelate. *Chem. Phys. Lett.* **2004**, *391*, 283–287.

31 Takeshima, M.; Matsui, A. H. Suppression and Enhancement of the Exciton-Phonon Interaction in Optical Absorption Spectra of Frenkel Exciton Microcrystallites. *J. Lumin.* **1999**, *82*, 195–204.

32 Patra, A.; Hebalkar, N.; Sreedhar, B.; Sarkar, M.; Samanta, A.; Radhakrishnan, T. P. Tuning the Size and Optical Properties in Molecular Nano/Microcrystals: Manifestation of Hierarchical Interactions. *Small* **2006**, *2*, 650–659.

33 Xiao, D.; Xi, L.; Yang, W.; Fu, H.; Shuai, Z.; Fang, Y.; Yao, J. Size-Tunable Emission from 1,3-Diphenyl-5-(2-anthryl)-2-pyrazoline Nanoparticles. *J. Am. Chem. Soc.* **2003**, *125*, 6740–6745, and references therein.

34 Lagoudakis, P. G.; de Souza, M. M.; Schindler, F.; Lupton, J. M.; Feldmann, J.; Wenus, J.; Lidzey, D. G. Experimental Evidence for Exciton Scaling Effects in Self-Assembled Molecular Wires. *Phys. Rev. Lett.* **2004**, *93*, 257401–257404.

35 Kurokawa, N.; Yoshikawa, H.; Hirota, N.; Hyodo, K.; Masuhara, H. Size-Dependent Spectroscopic Properties and Thermochromic Behavior in Poly(substituted thiophene) Nanoparticles. *ChemPhysChem* **2004**, *5*, 1609–1615.

36 (a) Hu, D.; Yu, J.; Wong, K.; Bagchi, B.; Rossky, P. J.; Barbara, P. F. Collapse of Stiff Conjugated Polymers with Chemical Defects into Ordered, Cylindrical Conformations. *Nature* **2000**, *405*, 1030–1033. (b) Grey, J. K.; Kim, D. Y.; Norris, B. C.; Miller, W. L.; Barbara, P. F. Size-Dependent Spectroscopic Properties of Conjugated Polymer Nanoparticles. *J. Phys. Chem. B* **2006**, *110*, 25568–25572, and references therein.

37 Asahi T.; Mashuara, H. Microspectroscpy of Single Nanoparticles. In *Single Organic Nanoparticles*; Masuhara, H., NakanishiH., Sasaki, K., Eds.; Springer: Berlin, 2003, 94–108.

38 Volkov, V. V.; Asahi, T.; Masuhara, H.; Masuhara, A.; Kasai, H.; Oikawa, H.; Nakanishi, H. Size-Dependent Optical Properties of Polydiacetylene Nanocrystal. *J. Phys. Chem. B* **2004**, *108*, 7674–7680.

39 Asahi, T.; Volkov, V. V.; Matsune, H.; Kawai H.; Masuhara, H. Spectroscopy and Photochemistry of Single Organic Nanocrystals Investigated by Using a Far-field Optical Microscope Coupled with an AFM System. In *Charge Transfer Processes in Semiconductor and Metal Nanostructures*; Rumbles, G.; Murakoshi, K.; Lian, T.; Eds. Electrochemical Society: Pennington, NJ, 2006; pp 150—161.

40 (a) Asahi, T.; Matsune, H.; Masuhara, H.; Kasai, H.; Nakanishi, H. Size-dependent Fluorescence Spectra of Individual Perylene Nanocrystals Studied by Far-Field Fluorescence Microspectroscopy Coupled with Atomic Force Microscope Observation. *Pol. J. Chem.* **2008**, *4*, 687–700. (b) Matsune, H.; Asahi, T.; Masuhara, H.; Kasai, H.; Nakanishi, H. Size-Effect on Fluorescence Spectrum of Perylene Nanocrystal Studied by Single-particle Microspectroscopy Coupled with Atomic Force Microscope Observation. *MRS Proc.* **2004**, *846*, DD10–DD18.

41 Gesquiere, A. J.; Uwada, T.; Asahi, T.; Masuhara, H.; Barbara, P. F. Single Molecule Spectroscopy of Organic Dye Nanoparticles. *Nano Lett.* **2005**, *5*, 1321–1325.

42 Hards, A.; Zhou, C.; Seitz, M.; Bräuchle, C.; Zumbusch, A. Simultaneous AFM Manipulation and Fluorescence Imaging of Single DNA Strands. *ChemPhysChem* **2005**, *6*, 534–540.

43 Oikawa, H.; Mitsui, T.; Onodera, T.; Kasai, H.; Nakanishi, H.; Sekiguchi, T. Crystal Size Dependence of Fluorescence Spectra from Perylene Nanocrystals Evaluated by Scanning Near-field Optical Microspectroscopy. *Jpn. J. Appl. Phys.* **2003**, *42*, L111–L113.

44 Niitsuma, J.-I.; Fujimura, T.; Itoh, T.; Kasai, H.; Okada, S.; Oikawa, H.; Nakanishi, H. Scanning Near-field Optical Microspectroscopy of Single Perylene Microcrystals. *Int. J. Mod. Phys. B* **2001**, *15*, 3901–3903.

45 Shen, Y.; Lin, T.-C.; Dai, J.; Markowicz, P.; Prasad, P. N. Near-field Optical Imaging of Transient Absorption Dynamics in Organic Nanocrystals. *J. Phys. Chem. B* **2003**, *107*, 13551–13553.

46 Barbara, P. F.; Adams, D. M.; O'connor, D. B. Imaging Organic Device Function with Near-field Scanning Optical Microscopy. *Annu. Rev. Mater. Sci.* **1999**, *29*, 433–439.

47 Brasselet, S.; Le Floc'h, V.; Treussart, F.; Roch, J.-F.; Zyss, J.; Botzung-Appert, E.; Ibanez, A. In Situ Diagnostics of the Crystalline Nature of Single Organic Nanocrystals by Nonlinear Microscopy. *Phys. Rev. Lett.* **2004**, *92*, 207401–207404.

48 Nishimura, H.; Yamaoka, T.; Mizuno, K.; Iemura, M.; Matsui, A. H. Luminescence of Free and Self-Trapped Excitons in α- and β-Perylene Crystals. *J. Phys. Soc. Jpn.* **1984**, *53*, 3999–4008.

49 Walker, B.; Port, H.; Wolf, H. C. The Two-Step Excimer Formation in Perylene Crystals. *Chem. Phys.* **1985**, *92*, 177.

50 Toyozawa, Y. Dynamics and Instabilities of an Exciton in the Phonon Field and the Correlated Absorption-Emission Spectra. *Pure Appl. Chem.* **1997**, *69*, 1171–1178.

51 Takagi, M. Electron-Diffraction Study of Liquid-Solid Transition of Thin Metal Films. *J. Phys. Soc. Jpn.* **1954**, *9*, 359–363.

52 Buffat, P.; Borel, L. P. Size Effect on the Melting Temperature of Gold Particles. *Phys. Rev. A* **1976**, *13*, 2287–2298.

53 Jackson, C. L.; Mckenna, G. B. The Melting Behavior of Organic Materials Confined in Porous Solids. *J. Chem. Phys.* **1997**, *93*, 9002–9011.

54 Anastas, P.; Horvath, I. T. Innovations and Green Chemistry. *Chem. Rev.* **2007**, *107*, 2169–2173.

55 (a) Jeon, H.-G.; Ryo, S.; Sugiyama, T.; Oh, I.; Masuhara, H.; Asahi, T. Fullerene (C60) Nanostructures Having Interpenetrating Surfaces Prepared by Electrophoretic Deposition of C60 Nanoparticles in Water. *Chem. Lett.* **2007**, *36*, 1160–1161. (b) Sugiyama, T.; Ryo, S.; Oh, I.; Asahi, T.; Masuhara, H. Preparation and Dispersibility of C60 Water Dispersion by Laser Ablation. Submitted to *J. Photoch. Photobio. A.*

56 Tabata, H.; Akamatsu, M.; Fujii, M.; Hayashi, S. Formation of C60 Colloidal Particles Suspended in Poor Solvent by Pulsed Laser Irradiation. *Jpn. J. Appl. Phys.* **2007**, *46*, 4338–4343.